Unraveling the molecular mechanism of interactions of the Rho GTPases Cdc42 and Rac1 with the scaffolding protein IQGAP2

Received for publication, December 21, 2017, and in revised form, January 12, 2018 Published, Papers in Press, January 22, 2018, DOI 10.1074/jbc.RA117.001596

E. Sila Ozdemir[‡1], Hyunbum Jang[§], Attila Gursoy[¶2], Ozlem Keskin[‡], Zhigang Li[‖], David B. Sacks[‖], and Ruth Nussinov[§3]**

*From the Departments of [‡]Chemical and Biological Engineering and [¶]Computer Engineering, Koc University, Istanbul 34450, Turkey, the [§]Cancer and Inflammation Program, Leidos Biomedical Research, Inc., Frederick National Laboratory for Cancer Research, NCI-Frederick, Frederick, Maryland 21702, the [‖]Department of Laboratory Medicine, National Institutes of Health, Bethesda, Maryland 20892, and the **Department of Human Molecular Genetics and Biochemistry, Sackler School of Medicine, Tel Aviv University, Tel Aviv 69978, Israel*

Edited by Karen G. Fleming

IQ motif–containing GTPase-activating proteins (IQGAPs) are scaffolding proteins playing central roles in cell–cell adhesion, polarity, and motility. The Rho GTPases Cdc42 and Rac1, in their GTP-bound active forms, interact with all three human IQGAPs. The IQGAP–Cdc42 interaction promotes metastasis by enhancing actin polymerization. However, despite their high sequence identity, Cdc42 and Rac1 differ in their interactions with IQGAP. Two Cdc42 molecules can bind to the Ex-domain and the RasGAP site of the GTPase-activating protein (GAP)-related domain (GRD) of IQGAP and promote IQGAP dimerization. Only one Rac1 molecule might bind to the RasGAP site of GRD and may not facilitate the dimerization, and the exact mechanism of Cdc42 and Rac1 binding to IQGAP is unclear. Using all-atom molecular dynamics simulations, site-directed mutagenesis, and Western blotting, we unraveled the detailed mechanisms of Cdc42 and Rac1 interactions with IQGAP2. We observed that Cdc42 binding to the Ex-domain of GRD of IQGAP2 (GRD2) releases the Ex-domain at the C-terminal region of GRD2, facilitating IQGAP2 dimerization. Cdc42 binding to the Ex-domain promoted allosteric changes in the RasGAP site, providing a binding site for the second Cdc42 in the RasGAP site. Of note, the Cdc42 "insert loop" was important for the interaction of the first Cdc42 with the Ex-domain. By contrast, differences in Rac1 insert-loop sequence and structure precluded its interaction with the Ex-domain. Rac1 could bind only to the RasGAP site of apo-GRD2 and could not facilitate IQGAP2 dimerization. Our detailed mechanistic insights help decipher how Cdc42 can stimulate actin polymerization in metastasis.

The Rho GTPase family is a subfamily of the Ras GTPase superfamily. Rho GTPases regulate multiple cellular processes, such as growth, survival, cell invasion, cell motility, and vesicle trafficking, by interacting with effector molecules (1–4). To date, the mammalian Rho GTPase family includes 22 members; Cdc42, Rac1, and RhoA are the most studied among them (5).

Rho GTPases are distinguished from other GTPases by the presence of an "insert loop," which is rich in charged residues in an α-helical motif (Fig. 1*A*). This α-helix is an important region for effector binding (6, 7). Rho GTPases share two common features that are crucial for their function: membrane anchorage and binary switch cycle (8). The GTPases can be located at the plasma membrane through their hypervariable region and a lipid anchor (9). The binary switch determines whether Rho GTPases are in the active or inactive state. The switch is on when GTP is bound and off when it is hydrolyzed to GDP. The GTP- and GDP-bound forms are referred to as the active and inactive states, respectively (10). Regulation of this switch cycle depends on two critical intrinsic reactions, GDP/GTP exchange and GTP hydrolysis (2, 11–13). Deregulation and alterations of Rho GTPases and the switch regulators may result in dysregulation of the cell cycle, which may affect cell morphogenesis, migration, adhesion, and oncogenesis (11, 14, 15).

The Rho GTPases Cdc42 and Rac1 have ~70% sequence identity, yet their functions in cellular processes differ (16, 17). Cdc42 plays a role in cytoskeletal rearrangement and cell motility. It facilitates the polarization of actin and microtubules and stimulates filopodium formation (18, 19). Rac1 regulates the formation of cortical actin-containing membrane ruffles and lamellipodia (20). Their activation upon GTP binding is

This work was supported in part by TUBITAK (Scientific and Technological Research Council of Turkey) Research Grant 114M196. This project was funded in whole or in part with Federal funds from the Frederick National Laboratory for Cancer Research, National Institutes of Health, under Contract HHSN261200800001E. This research was supported in part by the Intramural Research Program of National Institutes of Health, Frederick National Laboratory, Center for Cancer Research, and the Intramural Research Program of the National Institutes of Health Clinical Center. The authors declare that they have no conflicts of interest with the contents of this article. The content is solely the responsibility of the authors and does not necessarily represent the official views of the National Institutes of Health.

This article contains Figs. S1 and S2.

[1] Recipient of TUBITAK Scholarship 2211-E.

[2] To whom correspondence may be addressed: Dept. of Computer Engineering, Koc University, Istanbul 34450, Turkey. Tel.: 90-212-3381720; E-mail: agursoy@ku.edu.tr.

[3] To whom correspondence may be addressed: Cancer and Inflammation Program, NCI-Frederick, Leidos Biomedical Research, Inc., Frederick National Laboratory for Cancer Research, Frederick, MD 21702. Tel.: 301-846-5579; E-mail: nussinor@mail.nih.gov.

Downloaded from http://www.jbc.org/ by guest on April 10, 2019

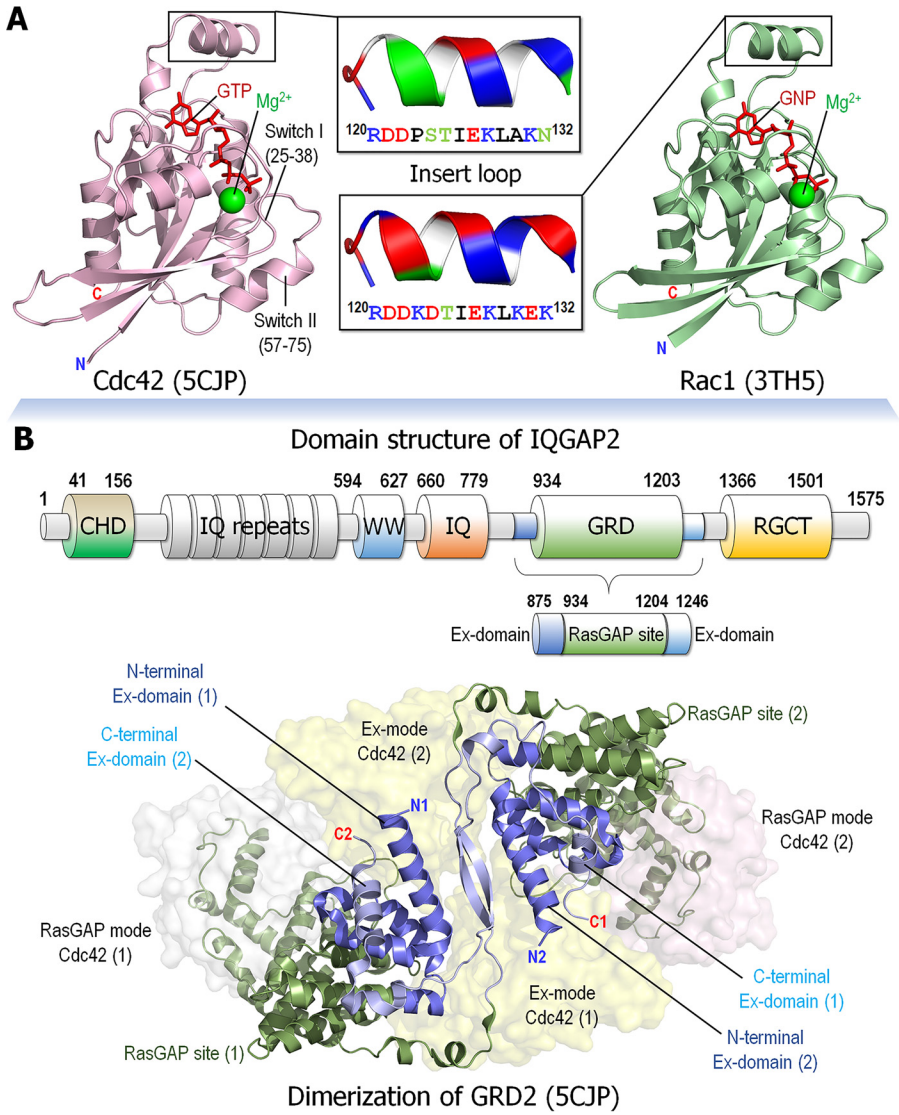


Figure 1. *A*, crystal structures of Cdc42 (PDB entry 5CJP, chain A) and Rac1 (PDB entry 3TH5). The insert loops in an α-helical motif from both proteins are highlighted. In the insert loop structure and sequence, hydrophobic, polar/glycine, positively charged, and negatively charged residues are *colored white* (*black*), *green*, *blue*, and *red*, respectively. *B*, domain structure of IQGAP2 and crystal structure of GRD of IQGAP2 (GRD2) dimer with four Cdc42 molecules (PDB entry 5CJP). Ex-domains form a dimerization interface, and the C-term of the Ex-domain intertwines with the counterpart C-term of the other GRD2. Each monomeric unit of GRD2 contains two Cdc42 molecules at the RasGAP site and the Ex-domain. The *number* in *parenthesis* denotes two monomeric units of GRD2.

accompanied by conformational changes in two regions, the switch I and II motifs (Fig. 1*A*). These regions serve as platforms for selective interactions with structurally and functionally diverse effectors, such as p21-activated kinase 1 (PAK1); p67phox, a member of the NADPH oxidase family; and IQ motif-containing GTPase-activating proteins (IQGAPs) (21, 22).

IQGAP is a ubiquitously expressed eukaryotic scaffold protein that is found in many species. The first identified and most-studied is human IQGAP1, a 189-kDa and 1657-amino acid–long protein (23). IQGAP1 plays a role in cell motility, cell–cell attachment, protein trafficking, transcription, regulation of the cytoskeleton, and microbial pathogenesis (24, 25). Cdc42 activity and intrinsic GTP hydrolysis are inhibited upon binding to IQGAPs, which stabilize its active form (26, 27). Cdc42 liberation fuels its signaling. Consistent with this, overexpression of IQGAP1 in mammalian cells promotes metastasis by stimulating actin polymerization mediated by Cdc42 (12, 15, 26, 28). In addition to Cdc42 and Rac1, IQGAPs interact with over 100 molecules, including calmodulin (CaM),[4] mitogen-activated protein kinase pathway proteins such as extracellular signal-regulated kinase 2 (ERK2), growth factors, chemokine receptors, actin, β-catenin, Yes-associated protein 1 (YAP1), small molecules such as Ca^{2+}, and more (23, 29–31). These interactions occur through five major domains of IQGAPs: the calponin homology domain for actin and Ca^{2+}-CaM binding, the

[4] The abbreviations used are: CaM, calmodulin; IQGAP, IQ motif–containing GTPase-activating protein; WASP, Wiskott–Aldrich syndrome protein; MD, molecular dynamics; C-term, C-terminal region of GRD2; RMSF, root mean square fluctuation; RMSD, root mean square deviation; WISP, weighted implementation of the suboptimal paths; H-bond, hydrogen bond; MM, molecular mechanics energies; GBSA, generalized Born surface area continuum solvation; CRIB, Cdc42/Rac binding; PVDF, polyvinylidene difluoride; PDB, Protein Data Bank.

Downloaded from http://www.jbc.org/ by guest on April 10, 2019

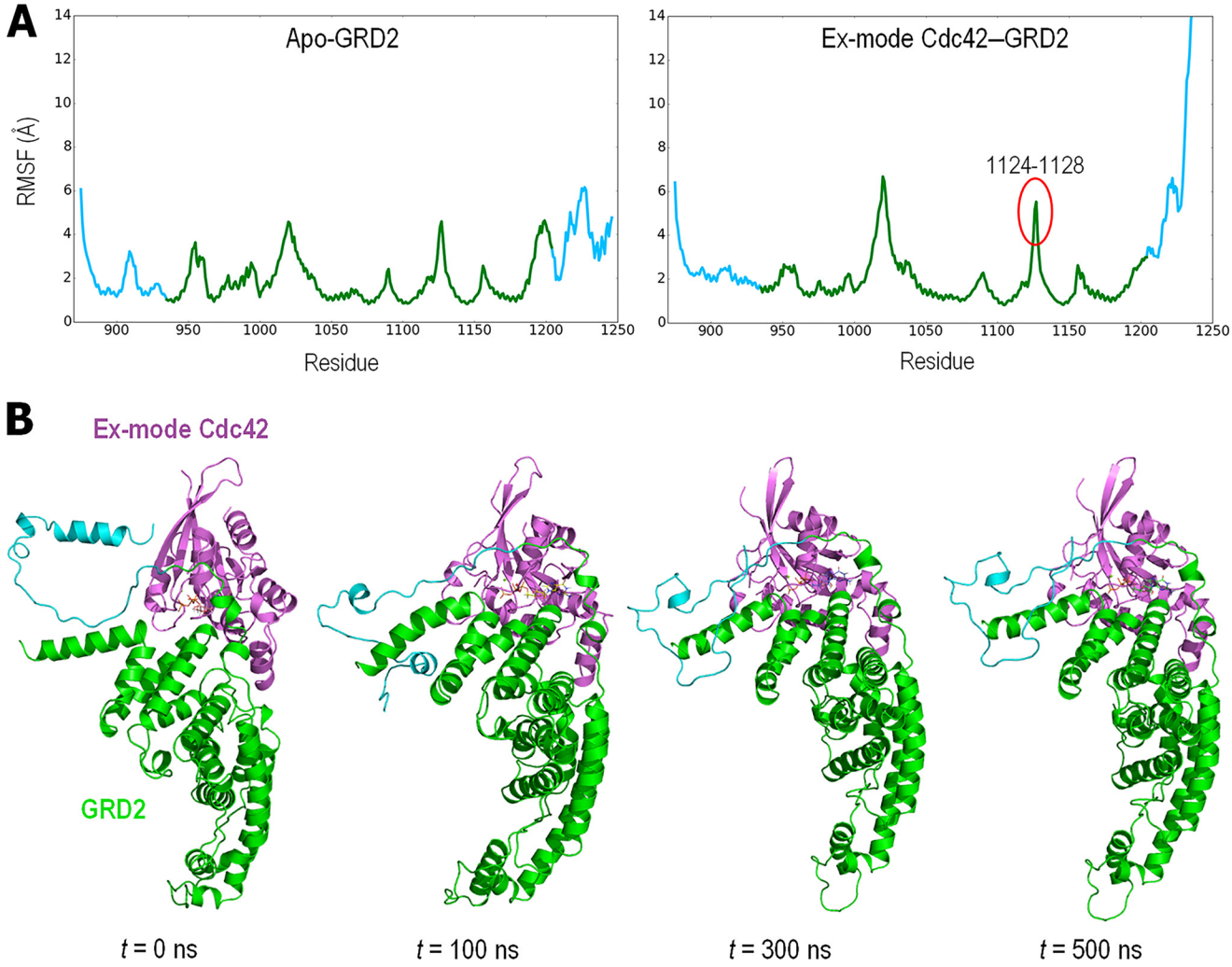


Figure 2. *A*, RMSF plots of apo-GRD2 (*left*) and GRD2 from Ex-mode Cdc42-GRD2 complex (*right*). *Green lines* cover the RasGAP site residues, and the remaining residues (*cyan lines*) belong to the Ex-domain. In the *right panel*, the *red ellipse* represents the residues between 1124 and 1128 that conformationally change upon Ex-mode Cdc42 binding. In the *right panel*, C-term residues show higher fluctuation than 10 Å (up to 20 Å); however, to clearly observe and compare fluctuation profiles of GRD2s from different complexes, the *y* axis limit is determined as 10 Å. *B*, time series of snapshots of Ex-mode Cdc42-GRD2. *Pink molecules* are Cdc42s, and *green molecules* are GRD2, whereas *cyan-highlighted residues* are the C-terms of the Ex-domain of GRD2s.

WW domain for ERK2 and phosphoinositide 3-kinase α binding, IQ motifs for CaM and myosin light chain binding, GRD for Cdc42 and Rac1 binding, and the RasGAP C-terminal domain for E-cadherin and β-catenin binding (32–35). Some of the binding partners compete or interfere with each other for binding to IQGAPs. For example, CaM binding causes allosteric Cdc42 release from GRD and decreases actin binding to the calponin homology domain (34). Free, active Cdc42 can then promote actin polymerization through Wiskott–Aldrich syndrome protein (WASP) and Arp2/3. IQGAP dimerization can also help to simultaneously bind to competing targets (36).

Despite the high degree of sequence identity, Cdc42 and Rac1 bind to IQGAP1 and IQGAP2 in different ways and perform distinct cellular functions. Two molecules of Cdc42 can bind to IQGAP1 and IQGAP2. The crystal structure of the GRD of IQGAP2 in complex with Cdc42 has been solved recently. The structure reveals two different Cdc42-binding sites in GRD2, the Ex-domain and the RasGAP sites (Fig. 1*B*) (16). The Ex-domain is composed of the N- and C-terminal regions of GRD2. Because IQGAP2 dimerization through GRD2s is promoted by Cdc42 binding, the complex has dimerized GRD2s and four Cdc42s bound to these GRD2s (16, 37). On the other hand, it was speculated that only one Rac1 molecule can bind to GRD, and there has been no evidence that it facilitates IQGAP dimerization (16); however, the exact mechanism of Rac1-GRD2 interaction and the differing stoichiometry have not been identified. If the assumption for Rac1-GRD interaction is correct, the reason behind the difference in binding of Cdc42 and Rac1 to GRD2 needs to be understood. To elucidate the mechanisms of these interactions, we carried out molecular dynamics (MD) simulations of Cdc42-GRD2 and Rac1-GRD2 complexes and performed site-directed mutagenesis and Western blot experiments to validate their predictions. We observed that the insert loop and switch I of Cdc42 are mainly responsible for Cdc42 binding to the Ex-domain. This binding releases the Ex-domain at the C-terminal region of GRD2 (hereafter referred to as C-term) to facilitate dimerization. However, the

Downloaded from http://www.jbc.org/ by guest on April 10, 2019

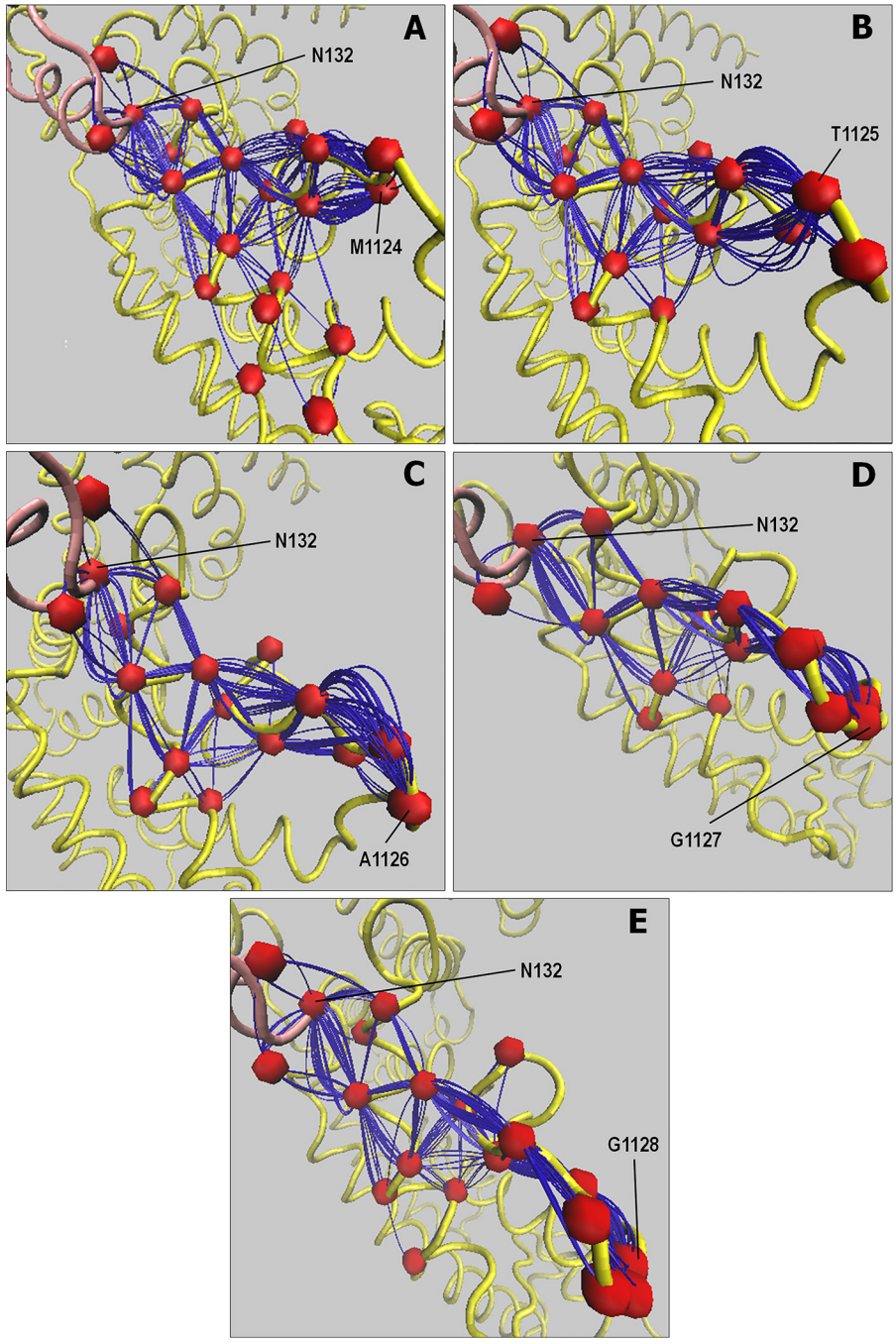


Figure 3. Allosteric pathways between Asn-132/Met-1124 (*A*), Asn-132/Thr-1125 (*B*), Asn-132/Ala-1126 (*C*), Asn-132/Gly-1127 (*D*), and Asn-132/Gly-1128 (*E*) of Ex-mode Cdc42 and GRD2 obtained by the WISP method. *Pink structures* are Cdc42s, and *yellow structures* are GRD2s. The *red balls* represent the residues involve in allosteric pathways, and the *blue lines* represent the possible paths followed by allosteric pathways.

orientation of the insert loop of Rac1 does not allow a Rac1–Ex-domain interaction; thus, the C-term cannot be released. Essentially, Cdc42 binding to the Ex-domain induces allosteric changes in the RasGAP site to enable the second Cdc42 to bind to this site, whereas apo-GRD2 is already available for Rac1 binding.

Here we unravel the underlying mechanism of the different stoichiometry that is involved in the binding of Cdc42 and Rac1 to GRD and of IQGAP2 dimerization. We then suggest how the mechanism can help to elucidate the key question of the roles of Cdc42 and Rac1 in actin polymerization in metastasis.

Results

Cdc42 insert-loop binding to the Ex-domain induces allosteric changes in the RasGAP site that facilitate GRD dimerization

The crystal structure of the GRD2 dimer bound to four Cdc42s (PDB entry 5CJP) provided a base structure for this study. In the structure, dimerization occurs between the Ex-domains of two GRD2s. Especially, the C-terminal portions

Downloaded from http://www.jbc.org/ by guest on April 10, 2019

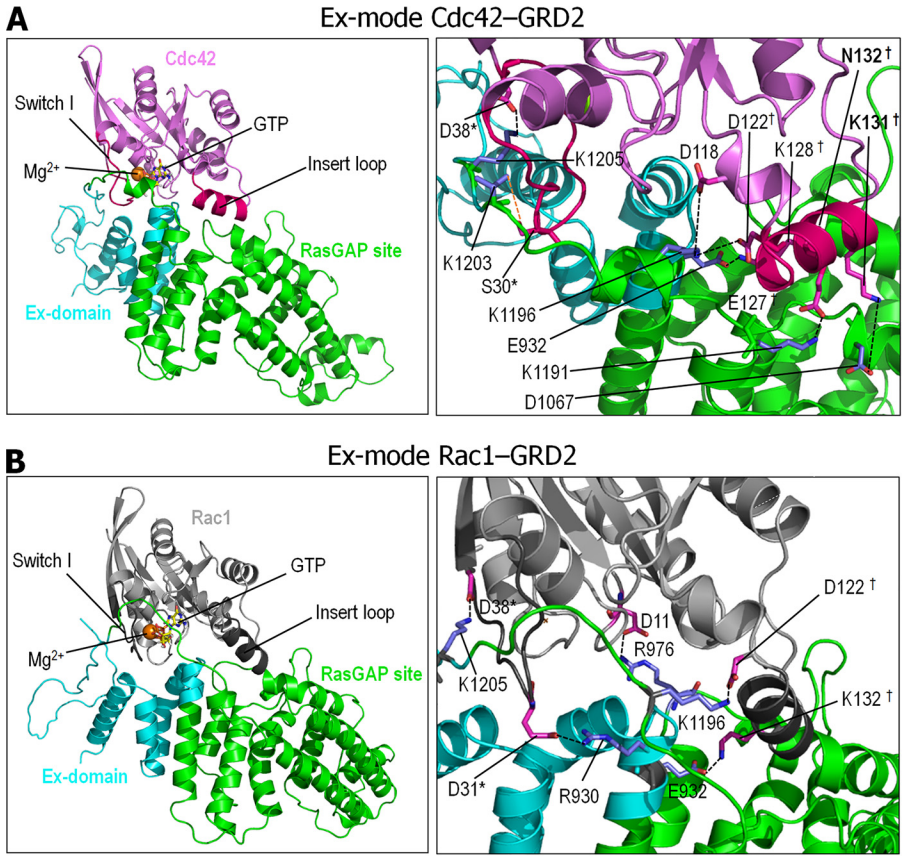


Figure 4. Interactions of Ex-mode Cdc42 (*A*) and Ex-mode Rac1 (*B*) with GRD2. On the *right-hand side*, stable salt bridges and stable H-bond formed between Ex-mode Cdc42 and GRD2 (*A*) and Ex-mode Rac1 and GRD2 (*B*) can be seen. *Green molecules* are GRD2, and pink/gray molecules are Cdc42/Rac1. *Dark pink/dark gray* regions are insert loops and switch I of Cdc42/Rac1. In the residue label, insert loop residues (†) and switch I residues (*) are indicated. *Black dashes*, salt bridges; *orange dashes*, H-bond. The residues Asn-132 and Lys-131 of Cdc42 are *highlighted* by *boldface type*.

(residues 1204–1246) are mainly involved in the dimerization, and they intertwine with each other (Fig. 1*B*).

Atomistic MD simulations were performed on the Ex-domain bound to the Cdc42 (hereafter referred to as Ex-mode Cdc42)-GRD2 complex for 500 ns. During the simulation, the bound C-term vigorously fluctuates compared with the C-term of apo-GRD2 (Fig. 2*A*, apo-GRD2 in the *left panel* and Ex-mode Cdc42–bound GRD2 in the *right panel*). Root mean square fluctuation (RMSF) calculations show that the residues in C-term (residues 1204–1246, *right panel* in Fig. 2*A*) fluctuate much more than the other residues of GRD2 upon Ex-mode Cdc42 binding. Because of this fluctuation, this region undergoes conformational changes; it is released and freely moves (Fig. 2*B*). Throughout the simulation, the C-term points in different directions. To confirm that the conformations with released C-term are highly populated throughout the Ex-mode Cdc42-GRD2 simulation, we performed clustering analysis with respect to the root mean square deviation (RMSD). We clustered the conformations based on pairwise best-fit RMSD. After the clustering analysis, we observed that C-term is released in 90% of the conformations (data not shown). This indicates that C-term–released conformations are highly populated throughout Ex-mode Cdc42-GRD2 simulation. These findings suggest that Cdc42-induced release of the C-term provides a platform for interacting with the C-term of the second GRD2 and facilitates dimerization.

In the crystal structure study, it was suggested that Ex-mode binding must precede Cdc42 binding to the RasGAP site (hereafter referred to as RasGAP mode Cdc42); however, how the binding of the first Cdc42 facilitates the binding of the second was unknown (16). Throughout our Ex-mode Cdc42-GRD2 simulation, as well as the fluctuation of C-term, we observed changes in the RasGAP site that enable the RasGAP mode Cdc42 binding. To elucidate how the binding of the Ex-mode Cdc42 allosterically affects the conformation of the RasGAP site, we conducted a dynamical network analysis using weighted implementation of the suboptimal paths (WISP) algorithm (38). The algorithm can identify the shortest primary communicating pathway through nodes that are protein residues of interest and edges connecting the nodes. In this analysis, we calculated 100 optimal pathways between selected residue pairs on Ex-mode Cdc42 and GRD2. The residue pair selection is made by considering residues that are in those regions that are mostly involved in the interactions and have high positive cross-correlation. We calculated the cross-correlation of the atomic fluctuations throughout the simulation. Positively correlated residues with a high correlation coefficient move in the same direction. We chose numerous residue pairs, but we could obtain pathways only between five of them. All possible pathways obtained by WISP start with Ex-mode Cdc42 residue Asn-132 and terminate at GRD2 residues 1124–1128 (Fig. 3), which have a high fluctuation profile (Fig. 2*A*, residues

Downloaded from http://www.jbc.org/ by guest on April 10, 2019

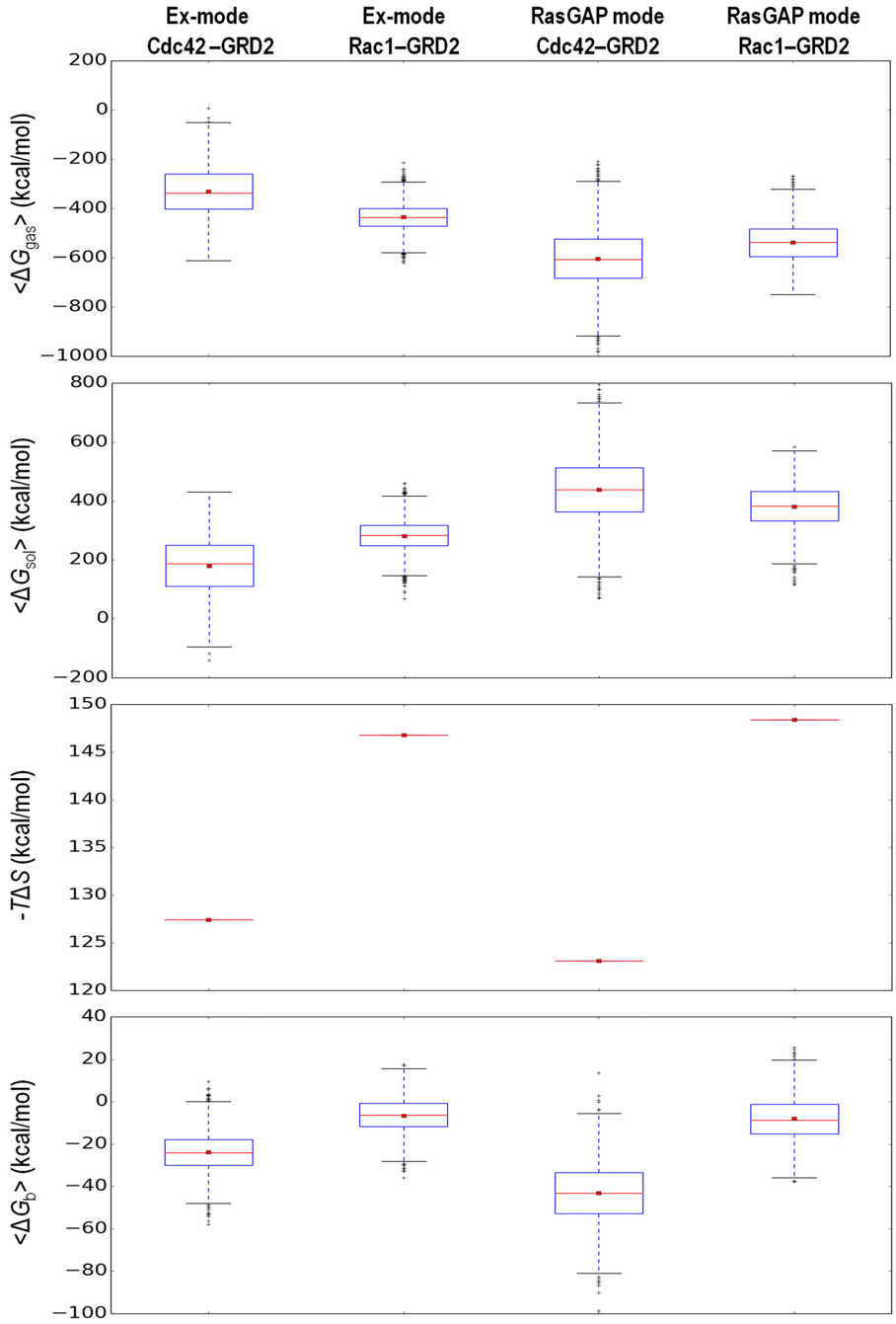


Figure 5. Binding free energies of Ex-mode Cdc42-GRD2, Ex-mode Rac1-GRD2, RasGAP mode Cdc42-GRD2, and RasGAP mode Rac1-GRD2 in kcal/mol calculated by the MM-GBSA method. In the calculation, gas phase contribution, $\langle \Delta G_{gas} \rangle$, the solvation energy contribution, $\langle \Delta G_{sol} \rangle$, and the entropic contribution, $-T\Delta S$, combine to give the average binding free energy, $\langle \Delta G_b \rangle$. In the box graphs, the *red dot* and *red line* denote the mean and median values, respectively. Whiskers above and below the box denote the 90th and 10th percentiles.

in *red ellipse*). The frequently involved residues in each of the 500 pathways (100 pathways for each five residue pairs) are Gln-983, Ile-1122, Arg-982, Asp-1123, and Ile-1121 of GRD2 (data not shown). Allosteric changes in residues 1124–1128 of GRD2, initiated by Asn-132 of Ex-mode Cdc42, prepare the RasGAP site for Cdc42 binding.

Rac1 cannot interact with the Ex-domain because of differences in sequence and orientation of its insert loop

Analysis of the interaction interface of Ex-mode Cdc42 with GRD2 identifies the regions and residues playing key roles. Stable salt bridges and hydrogen bonds (H-bonds) between Ex-mode Cdc42 and GRD2 generally involve insert-loop and switch I residues of Cdc42 (Fig. 4*A*). Residue Asn-132 of the insert loop, which is identified as the starting point of the allosteric changes in the RasGAP site, forms a stable hydrophilic interaction throughout the simulation that confirms its importance. Previous experimental studies also showed that Asn-132 residue plays an important role in the stability of Cdc42-GRD binding (6, 16). It has been shown that mutations in this residue significantly affect binding affinity of Cdc42 to GRD1 (6). Also, it has been reported that Asn-132 is involved in stable interac-

Downloaded from http://www.jbc.org/ by guest on April 10, 2019

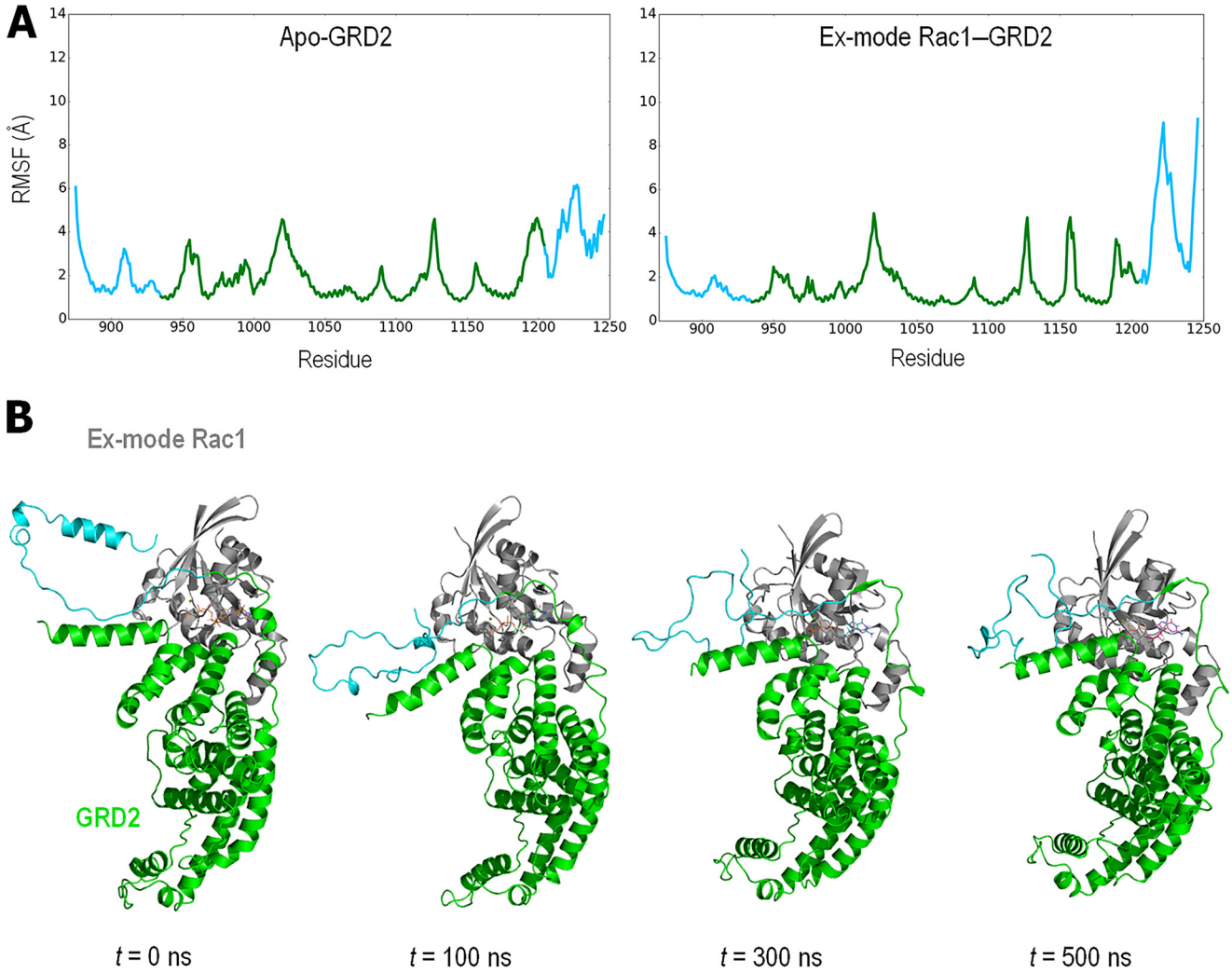


Figure 6. *A*, RMSF plots of apo-GRD2 (*left*) and GRD2 from Ex-mode Rac1-GRD2 complex (*right*). *Green lines* cover the RasGAP site residues, and the remaining residues (*cyan lines*) belong to the Ex-domain. *B*, time series of snapshots of Ex-mode Rac1-GRD2. *Gray molecules* are Rac1, and *green molecules* are GRD2, whereas *cyan-highlighted residues* are the C-terms of the Ex-domain of GRD2s.

tions with GRD2 (16). The insert loop is a Rho GTPase–specific α-helix structure, rich in both positively and negatively charged amino acids. This loop plays an important role in the interactions of Rho GTPases (6, 7). Taken together, this analysis suggests that the binding mechanism of Ex-mode Cdc42 to GRD2 exploits the highly charged insert loop and switch I residues and that this interaction, especially that involving residue Asn-132, induces allosteric changes in the RasGAP site to facilitate the RasGAP mode Cdc42 binding. The Ex-mode Cdc42-GRD2 interaction then allosterically releases the C-term and increases its fluctuation to induce GRD2 dimerization. We modeled the Ex-mode Rac1-GRD2 interaction using PRISM web server, which is a template-based protein-protein interaction prediction tool (39). 500-ns-long atomistic MD simulations were performed on the Ex-mode Rac1-GRD2 complex. We first observed that the orientation of the insert loop of Rac1 differs from that of Cdc42 (Fig. 4*B*, *left*). Because of this difference, fewer stable interactions formed between Rac1 and GRD2 compared with the Ex-mode Cdc42-GRD2 (Fig. 4*B*, *right*). Although some insert-loop residues are involved in salt-bridge and H-bond formation, stable Cdc42 interactions outnumber the stable Rac1 interactions. When we compared the structure and the sequence of Cdc42 and Rac1 in detail, we observed that there are some differences between the insert loops of Cdc42 and Rac1, both in sequence and structure. The sequence of the insert loop of Cdc42 is ^{120}RDDPSTIEKLAKN^{132}, and that of Rac1 is ^{120}RDDKDTIEKLKEK^{132} (Fig. 1*A*). There is a 38% difference between the sequences of the insert loops of Cdc42 and Rac1 (5 of the 13 amino acids differ). The polar Asn-132 residue of Cdc42 (Fig. 4*A*, *right*) was observed as an important residue in our analyses, inducing allosteric changes and involved in hydrophobic interaction; however, this residue is replaced with positively charged Lys-132 in Rac1. Previous experimental studies showed that mutating Asn-132 of Cdc42 to Lys decreases the affinity of Cdc42 for IQGAP1 (6). Also, positively charged Lys-131 in Cdc42, which forms a salt bridge with Asp-1067 of GRD2 (Fig. 4*A*, *right*), is replaced by negatively charged Glu-131 in Rac1. These two changes result in disruption of the stable interactions between Ex-mode Cdc42 and GRD2. The five different amino acids affect Rac1 interactions and change the structure of its insert loop. The allosteric effects induced by residue 132 of Cdc42 cannot be observed in the RasGAP site of

Downloaded from http://www.jbc.org/ by guest on April 10, 2019

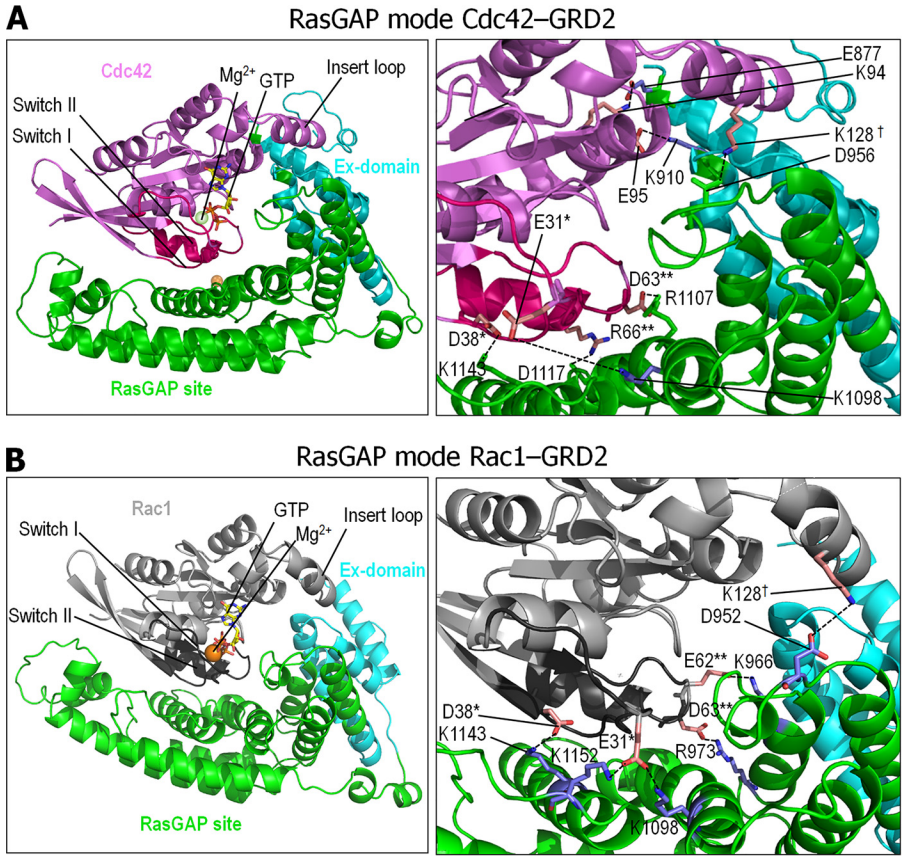


Figure 7. Interactions of RasGAP mode Cdc42 (*A*) and RasGAP mode Rac1 (*B*) with GRD2. On the *right-hand side*, stable salt bridges formed between RasGAP mode Cdc42 and GRD2 (*A*) and RasGAP mode Rac1 and GRD2 (*B*) can be seen. *Green molecules* are GRD2, and *pink/gray molecules* are Cdc42/Rac1. *Dark pink/dark gray regions* are switch I and switch II of Cdc42/Rac1. In the residue label, switch I residues (*) and switch II residues (**) are indicated. *Dashed lines*, salt bridges.

GRD2 after the Ex-mode Rac1 interaction. The changes in amino acid sequence in the Rac1 insert loop prevent it from inducing allosteric changes in the RasGAP site.

To compare the interaction strengths of these complexes, we calculated the binding free energy of Ex-mode Cdc42-GRD2 and Ex-mode Rac1-GRD2 using molecular mechanics energies combined with the generalized Born surface area continuum solvation (MM-GBSA) method (40). Our calculated binding free energies for the Ex-mode Cdc42-GRD2 and the Ex-mode Rac1-GRD2 interactions are -23.9 ± 9.2 and -6.6 ± 8.2 kcal/mol, respectively (Fig. 5). Compared with the Ex-mode Cdc42-GRD2 interaction, the Ex-mode Rac1-GRD2 interaction is significantly weaker, suggesting that because of the differences in the insert loop, Rac1 has a small number of residues involved in the intermolecular interaction with the Ex-domain of GRD2.

Consistent with these results, we could not observe release of the C-term throughout the simulation. Also, the fluctuation profile of GRD2 is similar to that of apo-GRD2 (Fig. 6*A*, *left*). Unlike the GRD2 from Ex-mode Cdc42-GRD2 complex (Fig. 2*A*, *right*), the C-term does not fluctuate vigorously (Fig. 6*A*, *right part* of the *right panel*). The C-term is not released but is folded inward, which closes the dimerization interface (Fig. 6*B*). Clustering analysis shows that the folded C-term conformation is highly populated throughout this simulation, and folded C-term populates 96.2% of all conformations (data not shown). As a result of this folding, exposure of the dimerization interface decreases, and the C-terms of the GRD2s cannot interact with each other. This finding also suggests that Rac1 cannot bind to the Ex-domain and cannot facilitate dimerization.

Cdc42 and Rac1 binding to the RasGAP site involve switch I and switch II residues and cannot induce C-term release

To observe the nature of RasGAP mode binding, we simulated RasGAP mode Cdc42-GRD2 complex. We observed that the binding mechanisms of Cdc42 to the RasGAP site of GRD2 are significantly different from those of Ex-mode Cdc42. In the case of the Ex-mode Cdc42-GRD2 interaction, the insert loop plays an important role in stabilizing the interaction (Fig. 4*A*). However, the insert loop of Cdc42 is less involved in the RasGAP mode Cdc42-GRD2 interaction (Fig. 7*A*). Instead, the salt bridges and H-bonds established between RasGAP mode Cdc42 and GRD2 mostly engage switch I and switch II residues. The binding mechanism of Rac1 to the RasGAP site of GRD2 shares similarities with the RasGAP mode Cdc42-GRD2 interaction, indicating that the RasGAP mode Rac1-GRD2 interaction also employs switch I and switch II residues (Fig. 7*B*). These findings also indicate that Rac1 can bind to the RasGAP site unlike the Ex-domain, because of stable interactions between RasGAP mode Rac1 and GRD2. Although binding free energy calculations imply that RasGAP mode Rac1 binding is weaker than RasGAP mode Cdc42 binding (-8.1 ± 10.2 kcal/

Downloaded from http://www.jbc.org/ by guest on April 10, 2019

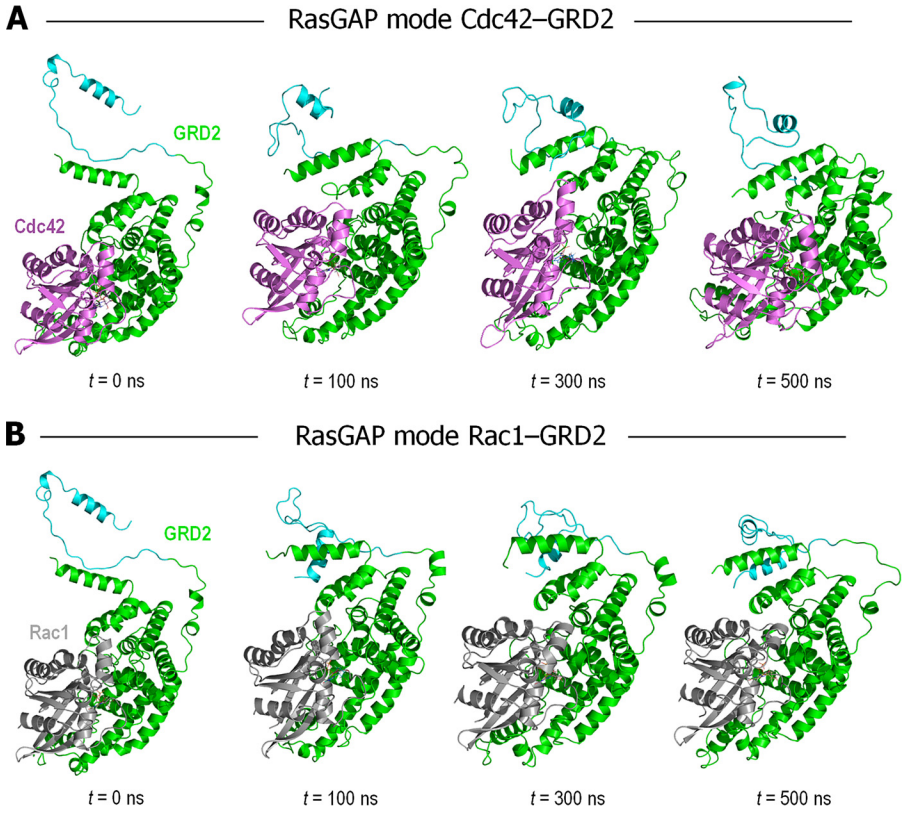


Figure 8. Time series of snapshots of RasGAP mode Cdc42-GRD2 (*A*) and RasGAP mode Rac1-GRD2 (*B*). *Pink molecules* are Cdc42, *gray molecules* are Rac1, and *green molecules* are GRD2, whereas *cyan-highlighted residues* are the C-terms of the Ex-domain of GRD2s.

mol *versus* −43.1 ± 14.1 kcal/mol, respectively; Fig. 5), the GRD2 structure that we used in the simulations (PDB entry 5CJP, chain E) is already allosterically changed and preorganized for the RasGAP mode Cdc42 binding. Nonetheless, our RasGAP mode Rac1-GRD2 simulation still provides a framework for this interaction.

Another similarity between RasGAP mode Cdc42 and Rac1 binding is the motion of the C-term. In both cases, we did not observe release of C-term, unlike in the case of Ex-mode Cdc42 binding, and a folded C-term appears throughout both simulations (Fig. 8). This indicates that the RasGAP mode binding of neither Cdc42 nor Rac1 is sufficient to induce C-term release and facilitate GRD2 dimerization. We conclude that Ex-mode Cdc42 binding is likely to be required for GRD dimerization, because this is the only case we observed that releases the C-term.

The Y1106A mutation causes complete loss of interactions of both Cdc42 and Rac1 with GRD2

We investigated energetically important residues in GRD2 to mutate and observe their effect on the Cdc42 and Rac1 binding. We observed that there are 10 hot spots, which are the residues contributing to the binding free energy most, in GRD2 using the HotRegion web server (41). We chose Tyr-1106 to mutate, because it has the highest pair potential among the other hot spot residues. Then we performed MD simulations after mutating *in silico* residue Tyr-1106 to alanine under the same conditions as the previous simulations of RasGAP mode Cdc42-GRD2 and RasGAP mode Rac1-GRD2 complexes. Because Tyr-1106 is a RasGAP site residue, we simulated RasGAP mode complexes. *In silico* mutations were performed using the "mutate" function of Discovery Studio version 4.1. We observed that the interaction of mutated GRD2 with Cdc42 and Rac1 is considerably weaker than the interaction of wildtype GRD2 (Fig. 9*A*). The binding free energy for RasGAP mode Cdc42-GRD2 (wildtype) interaction is −43.1 ± 14.1 kcal/mol; following mutation to alanine, it is −10.9 ± 11.5 kcal/mol. A similar decrease in binding strength is observed in the mutated RasGAP mode Rac1-GRD2 interaction; for the wildtype RasGAP mode Rac1-GRD2 interaction, it is −8.1 ± 10.2 kcal/mol, whereas for the mutant, it is 5.3 ± 11.8 kcal/mol. Also, in the mutated complexes, there are fewer stable salt bridges and H-bonds than in the wildtype interactions (Fig. 9, *B* and *C*). Tyr-1106 forms hydrophilic interactions in wildtype Cdc42-GRD2 and Rac1-GRD2 complexes. Additionally, upon mutation, stable interactions of some of the nearby residues observed in the wildtype simulations, such as Arg-1107 and Asp-956 (forming stable salt bridges with RasGAP Cdc42 residues (Fig. 7*A*)) and Asp-952 and Lys-966 (forming stable salt bridges with RasGAP Rac1 residues (Fig. 7*B*), are eliminated.

To validate the model, we generated a GST-tagged construct comprising the C-terminal half of IQGAP1 in which Tyr-1193 (which corresponds to Tyr-1106 in GRD2) was changed to Ala (termed Y1193A). We compared the abilities of the wildtype and the mutated IQGAP1 proteins to bind to purified Cdc42 and Rac1 *in vitro*. As observed previously by scintillation proximity assays (6), GST-pulldown analysis showed that the

Downloaded from http://www.jbc.org/ by guest on April 10, 2019

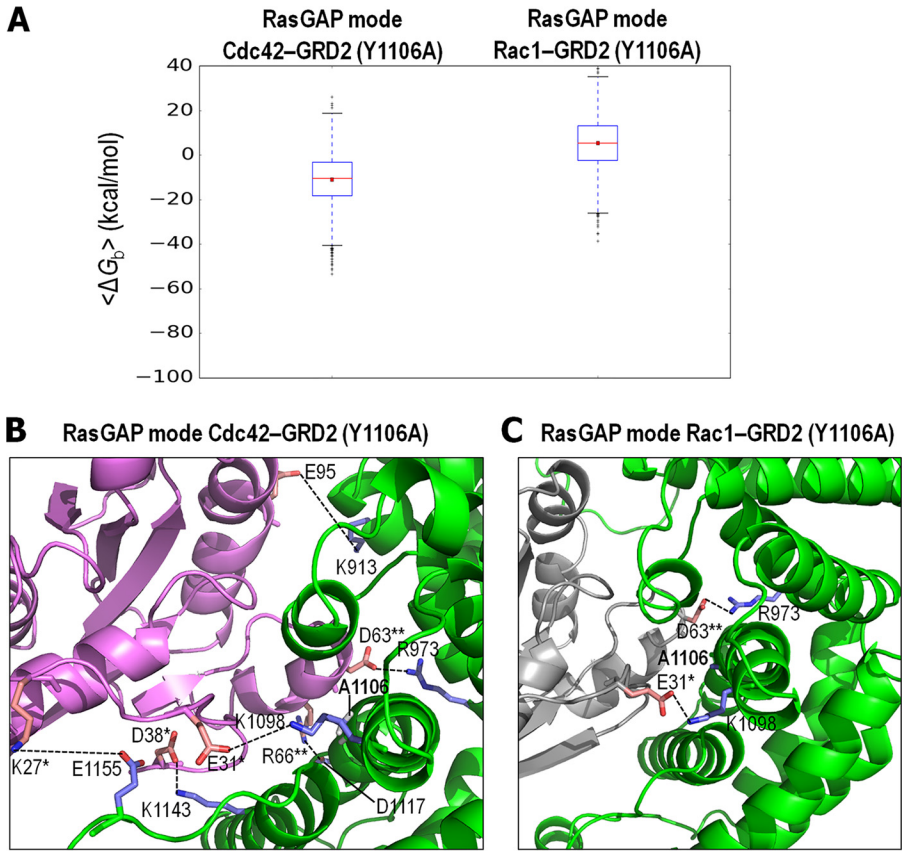


Figure 9. *A*, binding free energies of RasGAP mode Cdc42-GRD2^{Y1106A} and RasGAP mode Rac1-GRD2^{Y1106A} in kcal/mol calculated by the MM-GBSA method. *B* and *C*, stable salt bridges formed between RasGAP mode Cdc42 and GRD2^{Y1106A} (*B*) and RasGAP mode Rac1 and GRD2^{Y1106A} (*C*). *Green molecules* are GRD2, and *pink*/*gray molecules* are Cdc42/Rac1. In the residue label, switch I residues (*) and switch II residues (**) are indicated. *Dashed lines*, salt bridges. The mutated Ala-1106 residue is highlighted by *boldface type*.

C-terminal half of wildtype IQGAP1 binds Cdc42 and Rac1 (Fig. 10). By contrast, mutating a single amino acid (Tyr-1193) in IQGAP1 causes a complete loss of the Rac1-GRD1 interaction and markedly attenuates binding of Cdc42 to GRD1 (Fig. 10). Together, these data argue for the importance of the Tyr-1106 residue in IQGAP2 and provide a possible explanation for the complete loss of Cdc42 and Rac1 interactions with GRD2.

Discussion

Here, we provide possible mechanisms for the interactions of Cdc42 and Rac1 with GRD2 in atomistic detail (16). We observe that Cdc42 stably binds to the Ex-domain of GRD2 with high affinity, promoting high fluctuations of the C-term of the Ex-domain. The fluctuations release the C-term. The C-term plays a role in dimerization of IQGAP via its GRD. In GRD2s, they intertwine and stabilize the dimer structure; their release upon Cdc42 binding to the Ex-domain induces dimerization. Despite the availability of a crystal structure containing the GRD2 dimer and four molecules of Cdc42s that bind the Ex-domain and RasGAP site of each GRD2, the mechanism involving conformational changes facilitating the binding of the second Cdc42 was unclear. Through atomic-level conformations and allosteric pathway analysis, we showed that upon binding of Ex-mode Cdc42, allosteric changes are induced in the RasGAP site. These allosteric changes create a suitable binding interface for the binding of Cdc42 to the RasGAP site.

Rac1 is observed to only bind to the RasGAP site of GRD; however, it has been unclear whether Rac1 can bind to the Ex-domain and can promote dimerization (6, 42). When replacing Ex-mode Cdc42 with Rac1, with ~70% sequence identity, the C-term cannot be released; instead, it folds. The interaction interface for dimerization cannot be created when the C-term is folded; therefore, Rac1 cannot induce dimerization. Also, we do not observe allosteric changes in RasGAP site upon Ex-mode Rac1-GRD2 interaction. This is consistent with the observation that Rac1 can bind to the RasGAP site of apo-GRD2 and does not require allosteric changes to bind this site. Our energy calculations also showed that the binding affinity of Rac1 to the Ex-domain is considerably lower than the affinity of Cdc42 to the Ex-domain. Consistent with this, there are fewer stable interactions between Ex-mode Rac1 and GRD2 than between Ex-mode Cdc42 and GRD2. Detailed analysis indicates that the insert loop, which is Rho GTPase–specific and important for effector binding, plays a role in Cdc42–Ex-domain interaction. There are some sequence differences between the insert loops of Cdc42 and Rac1, which may decrease the interactions between Rac1 and the Ex-domain. All of these findings imply that Rac1 cannot interact with the Ex-domain and that neither facilitated dimerization nor allosteric changes are induced by

Downloaded from http://www.jbc.org/ by guest on April 10, 2019

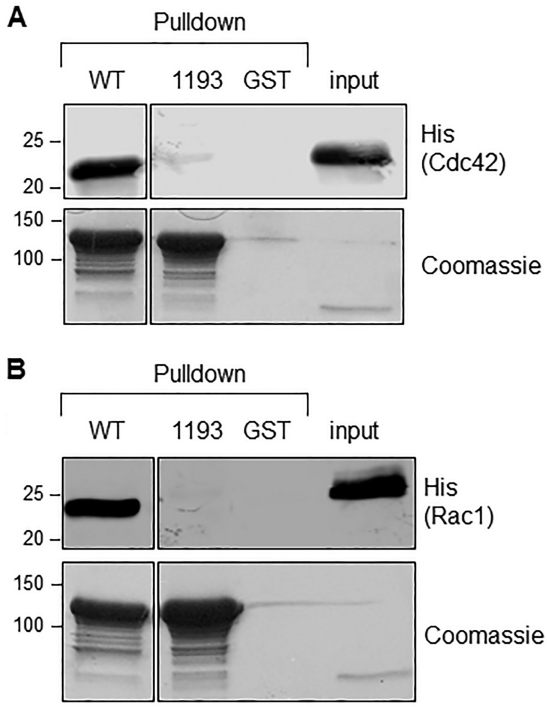


Figure 10. Mutation of Tyr-1193 of IQGAP1 impairs binding to Cdc42 and Rac1. 2 μg of purified His-Cdc42-Q61L (*A*) or His-Rac1-Q61L (*B*) was incubated with 3 μg of GST-IQGAP1-C (wildtype (*WT*) or Y1193A (*1193*)) on glutathione-Sepharose beads. Incubation with GST alone was used as a negative control. After incubation, samples were washed and resolved by SDS-PAGE. The top half of the gel (containing the GST-IQGAP1 constructs) was stained with Coomassie Blue. The bottom half of the gel, which contains Cdc42 or Rac1, was transferred to PVDF and probed with anti-His antibodies. Blots were imaged with Image Studio version 2.0 (LI-COR Biosciences). His-tagged Cdc42 or Rac1 that was not incubated with GST proteins was processed by SDS-PAGE and Western blotting (*Input*). The positions of migration of molecular weight markers are depicted. Data are representative of at least four independent experiments.

Rac1. These results support a 1:1 binding mode of Rac1 and GRD. They also explain the difference between the binding modes of Cdc42 and Rac1 by revealing the importance of the insert loop in the Ex-mode Cdc42-GRD2 interaction and show how (and possibly why) the insert loop of Rac1 differs from that of Cdc42.

Cdc42 and Rac1 are both known to bind to the RasGAP site of IQGAPs. However, the RasGAP site of apo-GRD2 provides a more suitable interaction interface for Rac1, whereas allosteric changes in RasGAP are required for RasGAP mode Cdc42 binding. Although their interaction interfaces on the RasGAP site differ, the Cdc42 and Rac1 interactions with the RasGAP site share some similarities. In both cases, a large number of stable interactions are formed, and these interactions mostly include switch I and switch II residues of Cdc42 and Rac1. Because these regions of Cdc42 and Rac1 are almost identical, these GTPases interact with the RasGAP site in a similar manner. Inducing C-term folding but not release is the other similarity in the RasGAP mode Cdc42 binding and RasGAP mode Rac1 binding. The C-term release that is observed in the case of the Ex-mode Cdc42-GRD2 interaction cannot be observed in any of the RasGAP mode binding. This suggests that Ex-mode Cdc42 binding induces dimerization by releasing the C-term; however, alone, RasGAP mode Cdc42 and RasGAP mode Rac1 binding are not sufficient to facilitate dimerization. With these findings, we also enhance understanding of IQGAP dimerization and provide an explanation as to why Cdc42, but not Rac1, can induce the dimerization.

Thus, the mechanism of the interactions of Cdc42 and Rac1 with GRD2 can now be understood. Our atomistic MD simulation data, combined with mutagenesis experiments, yield realistic models of Cdc42-GRD2 and Rac1-GRD2 interactions. The data provide insights into the mechanism of how Cdc42 can induce GRD2 dimerization and can allosterically change RasGAP site to create interaction interface for Cdc42 binding (Fig. 11*A*), whereas Rac1 can bind only to the RasGAP site and cannot facilitate dimerization (Fig. 11*B*). Cdc42 interaction with IQGAP is crucial because of their collective roles in cell motility (3, 4). IQGAP binds and stabilizes Cdc42 in its GTP-bound active form, blocking GTP hydrolysis (26).

Little is known about the detailed mechanisms of Cdc42 and Rac1 in actin polymerization (43, 44), although progress is being made (45). Their functions differ; Cdc42 enhances filopodia (containing parallel bundles of filamentous (F)-actin) formation, whereas Rac1 promotes lamellipodia (17, 46, 47). There is evidence that IQGAP1 is overexpressed in cancer, that it affects actin polymerization (48), and that it promotes migration of tumor cells (19). GTP-bound Cdc42 and IQGAP1 regulate filopodia formation. Cdc42 activates N-WASP by interacting with its Cdc42/Rac binding (CRIB) motif and releasing N-WASP's autoinhibited conformation; IQGAP1 C-terminal half activates N-WASP (49). Studies showed that Cdc42 and IQGAP1 bind to N-WASP and activate it synergistically (43). Activated N-WASP then recruits actin and Arp2/3, which nucleate filaments (3, 50). Cdc42-IQGAP binding stabilizes its active form, which facilitates Cdc42-dependent N-WASP activation. Actin polymerization by Rac1 differs, with lamellipodia (mesh) formation induced by Rac1 interaction with WAVE, a WASP-family verprolin homologous protein, and is not facilitated by IQGAP1 (51). Still, exactly how the different binding mechanisms of Cdc42 and Rac1 to IQGAP affect their actin-related functions is unclear. One possibility explored here is through stabilizing and releasing active Cdc42. It is possible that the 2:1 stoichiometry of Cdc42 binding to IQGAP1 is more stable than the 1:1 stoichiometry for Rac1. Which factor induces Cdc42 release from IQGAP and the mechanism regulating IQGAP1 binding to Cdc42 and Rac1 are also still open questions. Calmodulin may be one possibility.

To conclude, a major reason for the community focus on the Rho GTPases, particularly Cdc42 and Rac1, has been their effects on the actin cytoskeleton and thus tumor cell metastasis. However, exactly how they influence actin polymerization has been enigmatic. The emergence of the insert loop distinguishing them from the Ras family was established as critical, but the mechanism, mediated by IQGAP scaffolding protein, has been obscure. Here we provide a deeper understanding at the conformational level. Elucidating the interaction mechanism of Cdc42 with IQGAP is likely to facilitate targeting these molecules for therapeutic purposes.

Dynamic multiprotein assemblies shape the spatial structure of cell signaling (52, 53). Coordination, efficiency, and

Downloaded from http://www.jbc.org/ by guest on April 10, 2019

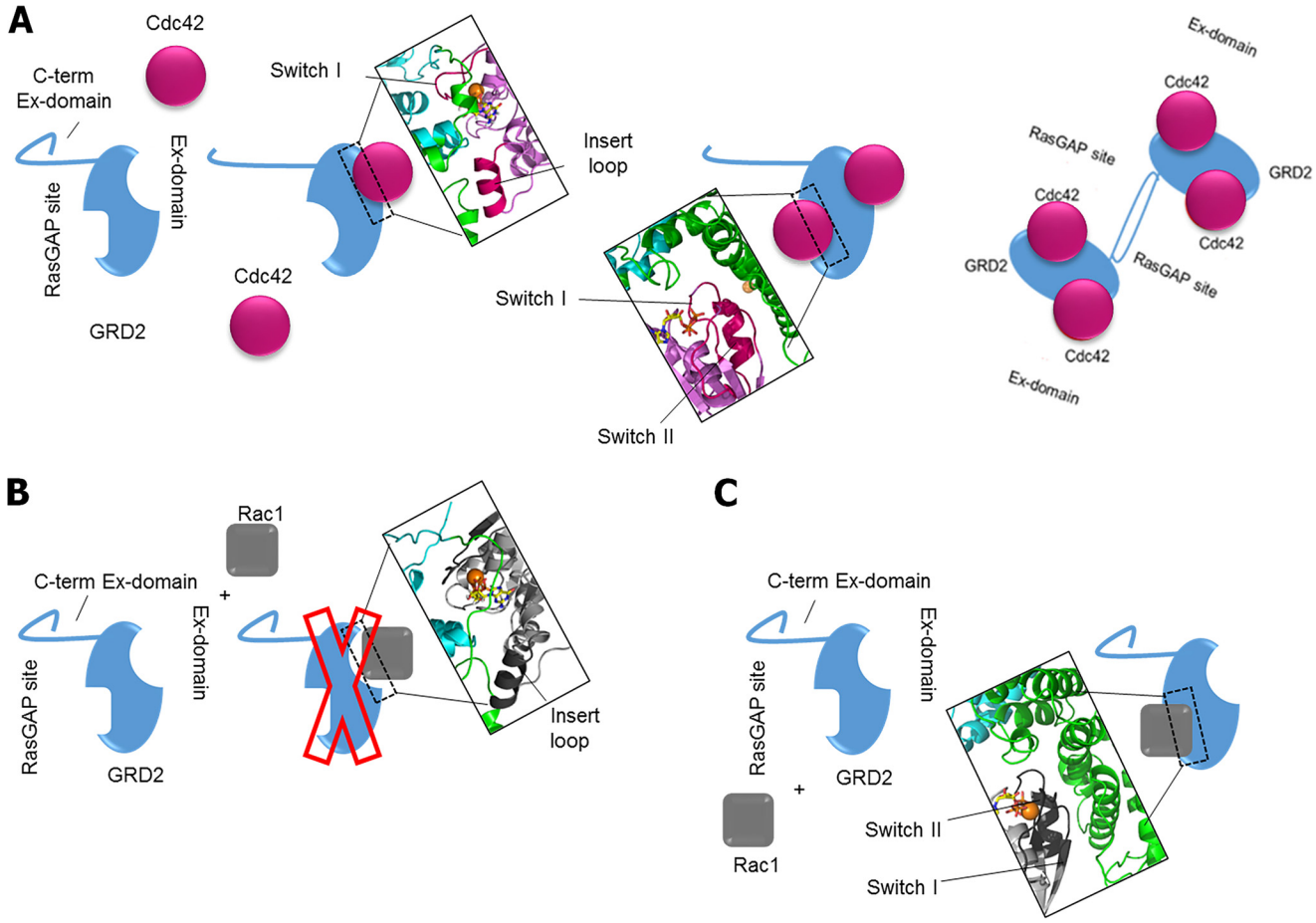


Figure 11. Interaction of GRD2 with Cdc42 (*A*) and Rac1 (*B* and *C*). *A*, *schematic diagram* illustrating the release of C-term and allosteric change in RasGAP site upon Ex-mode Cdc42 binding. Allosteric change in the RasGAP site induces binding of the second Cdc42 to RasGAP site, and GRD2 with two Cdc42s can dimerize. *B*, Rac1 cannot bind to the Ex-domain and cannot induce allosteric change in the RasGAP site and release of C-term. *C*, Rac1 can bind to the RasGAP site of apo-GRD2 but cannot induce the release of C-term. Therefore, Rac1 cannot facilitate GRD2 dimerization.

robustness are essential. IQGAP provides an exquisite example of how a scaffolding protein can carry out these tasks. Its dynamics and allosteric response not only link key pathways; they can also control pathway cross-talk and signaling by fine-tuning responses, in this case to distinct members of the same family, with key consequences for actin polymerization.

Experimental procedures

Initial configurations of Cdc42-GRD2 and Rac1-GRD2 complexes

The structure including four Cdc42s bound to GRD2 dimer (PDB entry 5CJP) was directly used to perform Ex-mode Cdc42-GRD2 (chain A and chain E) and RasGAP mode Cdc42-GRD2 (chain C and chain E) simulations. For Ex-mode Rac1-GRD2 and RasGAP mode Rac1-GRD2 complexes, the crystal structure of wildtype Rac1 (PDB entry 3TH5) was used. The structures were modeled using PRISM web server (39); the crystal structure of Cdc42-GRD2 (PDB entry 5CJP) was used as template, and we obtained initial configurations for Ex-mode Rac1-GRD2 and RasGAP Rac1-GRD2 complexes. GNP, a GTP analog bound to Rac1, was changed to GTP to be consistent with GTP-bound Cdc42-GRD2 complexes.

Atomistic MD simulations

A total of seven initial configurations were subject to the MD simulations in an aqueous environment; one apo-GRD2, two Cdc42-GRD2 complexes (Ex-mode Cdc42-GRD2 and RasGAP mode Cdc42-GRD2), two Rac1-GRD2 (Ex-mode Rac1-GRD2 and RasGAP mode Rac1-GRD2) complexes, one RasGAP mode Cdc42-mutated GRD2 (Y1106A) complex, and one RasGAP mode Rac1-mutated GRD2 (Y1106A) complex. The TIP3P water model was used to create the isometric unit cell box containing the protein complex.

Minimization was performed for 10,000 steps. In the production runs, the Langevin temperature control maintained the constant temperature at 310 K, and the pressure was kept at 1 atm. A total of 3.5 μs of simulations, each with 500 ns, were performed using the NAMD parallel-computing code (54) on a Biowulf cluster at the National Institutes of Health (Bethesda, MD) and on a yunus cluster at Koc University (Istanbul, Turkey). RMSD and free energy (ΔG) plots as a function of time show that 500-ns-long simulations are long enough to observe the behavior of our systems (Fig. S1 and Fig. S2). To exempt initial transients, the first 100-ns trajectories were removed, and thus averages were taken afterward. The simulated trajectories were analyzed using the CHARMM all-

Downloaded from http://www.jbc.org/ by guest on April 10, 2019

atom additive force field (version C36) programming package (55).

In addition to analyses performed using CHARMM, the WISP (38) plugin of VMD version 1.9.2 (56) and the Clustering function of Chimera version 1.10.2 (57) were used for allosteric pathway analysis and clustering analysis, respectively.

MM-GBSA calculations

The average binding free energy is calculated as follows,

$$\langle \Delta G_b \rangle = \langle \Delta G_{sol} \rangle + \langle \Delta G_{gas} \rangle - T\Delta S \quad \text{(Eq. 1)}$$

where $\langle \Delta G \rangle$ is the average binding free energy, ΔG_{sol} is the solvation energy contribution, ΔG_{gas} is the gas phase contribution, and $T\Delta S$ is the entropic contribution. Angle brackets represent the average along the simulations. The change in binding free energy due to the complex formation is calculated as follows.

$$\Delta G_b = G_b^{complex} - (G_b^{Cdc42/Rac1} + G_b^{GRD2}) \quad \text{(Eq. 2)}$$

Further details of the calculation protocol have been reported in our previous studies (58). The electrostatic and non-polar contributions to the solvation free energy are obtained from the GB approximation within the CHARMM program (55).

Protein expression and purification

The generation of the GST-tagged C-terminal half of IQGAP1 (IQGAP1-C, amino acids 864–1657) has been described previously (34). IQGAP1-C with Tyr-1193 mutated to Ala (Y1193A) was generated using site-directed mutagenesis. His-Cdc42-Q61L and His-Rac1-Q61L (constitutively active forms of Cdc42 and Rac1, respectively) were generated from pGEX-Cdc42-Q61L and pGEX-Rac1-Q61L (residues 1–184 for Cdc42 and 1–192 for Rac1; generously donated by Darerca Owen, University of Cambridge, Cambridge, UK) by excising them and inserting the plasmids into pRSET. DNA sequencing confirmed the sequences of the constructs. The GST fusion proteins were expressed in *Escherichia coli* and isolated using glutathione-Sepharose (GE Healthcare) chromatography essentially as described previously (34). His-Cdc42-Q61L and His-Rac1-Q61L were purified with nickel-nitrilotriacetic acid–agarose (Qiagen), following the company's protocol. The size and purity of the GST- and His-tagged proteins were evaluated by SDS-PAGE and Coomassie staining. All of the proteins migrated to the expected positions on SDS-PAGE and were at least 90% pure.

In vitro binding assay

Purified His-Cdc42-Q61L or His-Rac1-Q61L (2 μg each) in 1 ml of Buffer A (50 mM Tris-HCl, pH 7.4, 150 mM NaCl, 1% Triton X-100, and 1 mM PMSF) was precleared with 40 μl of glutathione-Sepharose beads. After incubating for 1 h at 4 °C, the beads were removed, and 3 μg of wildtype GST-IQGAP1-C or GST-IQGAP1-C Y1193A (prebound to glutathione-Sepharose) was added. His-Cdc42-Q61L or His-Rac1-Q61L was incubated with GST bound to glutathione-Sepharose as a negative control. Samples were rotated for 3 h at 4 °C, washed five times with Buffer A, and then resolved by SDS-PAGE. The gel was cut at the 50 kDa region. The upper portion of the gel was stained with Coomassie Blue. The lower portion of the gel was transferred to PVDF. The PVDF membrane was probed with anti-His antibody (His-probe (H-3) sc-8036, mouse monoclonal IgG, Santa Cruz Biotechnology, Inc.) and imaged with the Odyssey Imaging System (LI-COR Biosciences) essentially as described previously (59).

Author contributions—E. S. O., H. J., D. B. S., and R. N. conceptualization; E. S. O., H. J., O. K., and Z. L. data curation; E. S. O. formal analysis; E. S. O. and H. J. investigation; E. S. O. writing-original draft; H. J., A. G., O. K., D. B. S., and R. N. supervision; H. J., A. G., O. K., D. B. S., and R. N. writing-review and editing; A. G. software; O. K. resources; E. S. O. and Z. L. methodology.

Acknowledgments—All simulations were performed using the high-performance computational facilities of the Biowulf PC/Linux cluster at the National Institutes of Health (Bethesda, MD) and yunus cluster at Koc University (Istanbul, Turkey). We thank Tsung-Jen Liao from the Nussinov group for help with the WISP method and Laetitia Gorisse and Andrew Hedman from the Sacks laboratory for help with the experimental figure. We thank the members of the Nussinov group and the Sacks laboratory for insightful discussion.

References

1. Boguski, M. S., and McCormick, F. (1993) Proteins regulating Ras and its relatives. *Nature* **366,** 643–654 CrossRef Medline
2. Sahai, E., and Marshall, C. J. (2002) RHO-GTPases and cancer. *Nat. Rev. Cancer* **2,** 133–142 CrossRef Medline
3. Ridley, A. J. (2001) Rho family proteins: coordinating cell responses. *Trends Cell Biol.* **11,** 471–477 CrossRef Medline
4. Tapon, N., and Hall, A. (1997) Rho, Rac and Cdc42 GTPases regulate the organization of the actin cytoskeleton. *Curr. Opin. Cell Biol.* **9,** 86–92 CrossRef Medline
5. Rojas, A. M., Fuentes, G., Rausell, A., and Valencia, A. (2012) The Ras protein superfamily: evolutionary tree and role of conserved amino acids. *J. Cell Biol.* **196,** 189–201 CrossRef Medline
6. Owen, D., Campbell, L. J., Littlefield, K., Evetts, K. A., Li, Z., Sacks, D. B., Lowe, P. N., and Mott, H. R. (2008) The IQGAP1-Rac1 and IQGAP1-Cdc42 interactions: interfaces differ between the complexes. *J. Biol. Chem.* **283,** 1692–1704 CrossRef Medline
7. Zong, H., Kaibuchi, K., and Quilliam, L. A. (2001) The insert region of RhoA is essential for Rho kinase activation and cellular transformation. *Mol. Cell. Biol.* **21,** 5287–5298 CrossRef Medline
8. Dvorsky, R., and Ahmadian, M. R. (2004) Always look on the bright site of Rho: structural implications for a conserved intermolecular interface. *EMBO Rep.* **5,** 1130–1136 CrossRef Medline
9. Lam, B. D., and Hordijk, P. L. (2013) The Rac1 hypervariable region in targeting and signaling: a tail of many stories. *Small GTPases* **4,** 78–89 CrossRef Medline
10. Rathinam, R., Berrier, A., and Alahari, S. K. (2011) Role of Rho GTPases and their regulators in cancer progression. *Front. Biosci.* **16,** 2561–2571 CrossRef Medline
11. Barbacid, M. (1990) *ras* oncogenes: their role in neoplasia. *Eur J. Clin. Invest.* **20,** 225–235 Medline
12. Casteel, D. E., Turner, S., Schwappacher, R., Rangaswami, H., Su-Yuo, J., Zhuang, S., Boss, G. R., and Pilz, R. B. (2012) Rho isoform-specific interaction with IQGAP1 promotes breast cancer cell proliferation and migration. *J. Biol. Chem.* **287,** 38367–38378 CrossRef Medline
13. Gideon, P., John, J., Frech, M., Lautwein, A., Clark, R., Scheffler, J. E., and Wittinghofer, A. (1992) Mutational and kinetic analyses of the GTPase-activating protein (GAP)-p21 interaction: the C-terminal domain of GAP is not sufficient for full activity. *Mol. Cell. Biol.* **12,** 2050–2056 CrossRef Medline

Downloaded from http://www.jbc.org/ by guest on April 10, 2019

14. Etienne-Manneville, S., and Hall, A. (2002) Rho GTPases in cell biology. *Nature* **420,** 629–635 CrossRef Medline
15. Zandvakili, I., Lin, Y., Morris, J. C., and Zheng, Y. (2017) Rho GTPases: anti- or pro-neoplastic targets? *Oncogene* **36,** 3213–3222 Medline
16. LeCour, L., Jr., Boyapati, V. K., Liu, J., Li, Z., Sacks, D. B., and Worthylake, D. K. (2016) The structural basis for Cdc42-induced dimerization of IQGAPs. *Structure* **24,** 1499–1508 CrossRef Medline
17. Hall, A. (1998) Rho GTPases and the actin cytoskeleton. *Science* **279,** 509–514 CrossRef Medline
18. Stowers, L., Yelon, D., Berg, L. J., and Chant, J. (1995) Regulation of the polarization of T cells toward antigen-presenting cells by Ras-related GTPase CDC42. *Proc. Natl. Acad. Sci. U.S.A.* **92,** 5027–5031 CrossRef Medline
19. Mataraza, J. M., Briggs, M. W., Li, Z., Entwistle, A., Ridley, A. J., and Sacks, D. B. (2003) IQGAP1 promotes cell motility and invasion. *J. Biol. Chem.* **278,** 41237–41245 CrossRef Medline
20. Jaffe, A. B., and Hall, A. (2005) Rho GTPases: biochemistry and biology. *Annu. Rev. Cell Dev. Biol.* **21,** 247–269 CrossRef Medline
21. Lapouge, K., Smith, S. J., Walker, P. A., Gamblin, S. J., Smerdon, S. J., and Rittinger, K. (2000) Structure of the TPR domain of p67phox in complex with Rac.GTP. *Mol. Cell* **6,** 899–907 CrossRef Medline
22. Watanabe, T., Wang, S., and Kaibuchi, K. (2015) IQGAPs as key regulators of actin-cytoskeleton dynamics. *Cell Struct. Funct.* **40,** 69–77 CrossRef Medline
23. Weissbach, L., Settleman, J., Kalady, M. F., Snijders, A. J., Murthy, A. E., Yan, Y. X., and Bernards, A. (1994) Identification of a human rasGAP-related protein containing calmodulin-binding motifs. *J. Biol. Chem.* **269,** 20517–20521 Medline
24. Briggs, M. W., and Sacks, D. B. (2003) IQGAP proteins are integral components of cytoskeletal regulation. *EMBO Rep.* **4,** 571–574 CrossRef Medline
25. Tanos, B. E., Yeaman, C., and Rodriguez-Boulan, E. (2016) An emerging role for IQGAP1 in tight junction control. *Small GTPases*, 1–9 CrossRef Medline
26. Swart-Mataraza, J. M., Li, Z. G., and Sacks, D. B. (2002) IQGAP1 is a component of Cdc42 signaling to the cytoskeleton. *J. Biol. Chem.* **277,** 24753–24763 CrossRef Medline
27. Kuroda, S., Fukata, M., Nakagawa, M., Fujii, K., Nakamura, T., Ookubo, T., Izawa, I., Nagase, T., Nomura, N., Tani, H., Shoji, I., Matsuura, Y., Yonehara, S., and Kaibuchi, K. (1998) Role of IQGAP1, a target of the small GTPases Cdc42 and Rac1, in regulation of E-cadherin-mediated cell-cell adhesion. *Science* **281,** 832–835 CrossRef Medline
28. Brown, M. D., and Sacks, D. B. (2006) IQGAP1 in cellular signaling: bridging the GAP. *Trends Cell Biol.* **16,** 242–249 CrossRef Medline
29. Cheung, K. L., Lee, J. H., Shu, L., Kim, J. H., Sacks, D. B., and Kong, A. N. (2013) The Ras GTPase-activating-like protein IQGAP1 mediates Nrf2 protein activation via the mitogen-activated protein kinase/extracellular signal-regulated kinase (ERK) kinase (MEK)-ERK pathway. *J. Biol. Chem.* **288,** 22378–22386 CrossRef Medline
30. Jameson, K. L., Mazur, P. K., Zehnder, A. M., Zhang, J., Zarnegar, B., Sage, J., and Khavari, P. A. (2013) IQGAP1 scaffold-kinase interaction blockade selectively targets RAS-MAP kinase-driven tumors. *Nat. Med.* **19,** 626–630 CrossRef Medline
31. Smith, J. M., Hedman, A. C., and Sacks, D. B. (2015) IQGAPs choreograph cellular signaling from the membrane to the nucleus. *Trends Cell Biol.* **25,** 171–184 CrossRef Medline
32. Brill, S., Li, S., Lyman, C. W., Church, D. M., Wasmuth, J. J., Weissbach, L., Bernards, A., and Snijders, A. J. (1996) The Ras GTPase-activating-protein-related human protein IQGAP2 harbors a potential actin binding domain and interacts with calmodulin and Rho family GTPases. *Mol. Cell. Biol.* **16,** 4869–4878 CrossRef Medline
33. Roy, M., Li, Z., and Sacks, D. B. (2004) IQGAP1 binds ERK2 and modulates its activity. *J. Biol. Chem.* **279,** 17329–17337 CrossRef Medline
34. Ho, Y. D., Joyal, J. L., Li, Z., and Sacks, D. B. (1999) IQGAP1 integrates Ca^{2+}/calmodulin and Cdc42 signaling. *J. Biol. Chem.* **274,** 464–470 CrossRef Medline
35. Hart, M. J., Callow, M. G., Souza, B., and Polakis, P. (1996) IQGAP1, a calmodulin-binding protein with a rasGAP-related domain, is a potential effector for cdc42Hs. *EMBO J.* **15,** 2997–3005 Medline
36. Marianayagam, N. J., Sunde, M., and Matthews, J. M. (2004) The power of two: protein dimerization in biology. *Trends Biochem. Sci.* **29,** 618–625 CrossRef Medline
37. Ren, J. G., Li, Z., Crimmins, D. L., and Sacks, D. B. (2005) Self-association of IQGAP1: characterization and functional sequelae. *J. Biol. Chem.* **280,** 34548–34557 CrossRef Medline
38. Van Wart, A. T., Durrant, J., Votapka, L., and Amaro, R. E. (2014) Weighted implementation of suboptimal paths (WISP): an optimized algorithm and tool for dynamical network analysis. *J. Chem. Theory Comput.* **10,** 511–517 CrossRef Medline
39. Baspinar, A., Cukuroglu, E., Nussinov, R., Keskin, O., and Gursoy, A. (2014) PRISM: a web server and repository for prediction of protein-protein interactions and modeling their 3D complexes. *Nucleic Acids Res.* **42,** W285–W289 CrossRef Medline
40. Sun, H., Li, Y., Tian, S., Xu, L., and Hou, T. (2014) Assessing the performance of MM/PBSA and MM/GBSA methods. 4. Accuracies of MM/PBSA and MM/GBSA methodologies evaluated by various simulation protocols using PDBbind data set. *Phys. Chem. Chem. Phys.* **16,** 16719–16729 CrossRef Medline
41. Cukuroglu, E., Gursoy, A., and Keskin, O. (2012) HotRegion: a database of predicted hot spot clusters. *Nucleic acids research* **40,** D829–D833 CrossRef Medline
42. Nouri, K., Fansa, E. K., Amin, E., Dvorsky, R., Gremer, L., Willbold, D., Schmitt, L., Timson, D. J., and Ahmadian, M. R. (2016) IQGAP1 interaction with RHO family proteins revisited: kinetic and equilibrium evidence for multiple distinct binding sites. *J. Biol. Chem.* **291,** 26364–26376 CrossRef Medline
43. Le Clainche, C., Schlaepfer, D., Ferrari, A., Klingauf, M., Grohmanova, K., Veligodskiy, A., Didry, D., Le, D., Egile, C., Carlier, M. F., and Kroschewski, R. (2007) IQGAP1 stimulates actin assembly through the N-WASP-Arp2/3 pathway. *J. Biol. Chem.* **282,** 426–435 CrossRef Medline
44. Etienne-Manneville, S. (2004) Actin and microtubules in cell motility: which one is in control? *Traffic* **5,** 470–477 CrossRef Medline
45. Kazanietz, M. G., and Caloca, M. J. (2017) The Rac GTPase in cancer: from old concepts to new paradigms. *Cancer Res.* **77,** 5445–5451 CrossRef Medline
46. Burridge, K., and Wennerberg, K. (2004) Rho and Rac take center stage. *Cell* **116,** 167–179 CrossRef Medline
47. Carlier, M. F., and Shekhar, S. (2017) Global treadmilling coordinates actin turnover and controls the size of actin networks. *Nat. Rev. Mol. Cell Biol.* **18,** 389–401 CrossRef Medline
48. Bashour, A. M., Fullerton, A. T., Hart, M. J., and Bloom, G. S. (1997) IQGAP1, a Rac- and Cdc42-binding protein, directly binds and cross-links microfilaments. *J. Cell Biol.* **137,** 1555–1566 CrossRef Medline
49. Benseñor, L. B., Kan, H. M., Wang, N., Wallrabe, H., Davidson, L. A., Cai, Y., Schafer, D. A., and Bloom, G. S. (2007) IQGAP1 regulates cell motility by linking growth factor signaling to actin assembly. *J. Cell Sci.* **120,** 658–669 CrossRef Medline
50. Leung, T., Chen, X. Q., Tan, I., Manser, E., and Lim, L. (1998) Myotonic dystrophy kinase-related Cdc42-binding kinase acts as a Cdc42 effector in promoting cytoskeletal reorganization. *Mol. Cell. Biol.* **18,** 130–140 CrossRef Medline
51. Heasman, S. J., and Ridley, A. J. (2008) Mammalian Rho GTPases: new insights into their functions from *in vivo* studies. *Nat. Rev. Mol. Cell Biol.* **9,** 690–701 CrossRef Medline
52. Nussinov, R., and Jang, H. (2014) Dynamic multiprotein assemblies shape the spatial structure of cell signaling. *Prog. Biophys. Mol. Biol.* **116,** 158–164 CrossRef Medline
53. Nussinov, R., Ma, B., and Tsai, C. J. (2013) A broad view of scaffolding suggests that scaffolding proteins can actively control regulation and signaling of multienzyme complexes through allostery. *Biochim. Biophys. Acta* **1834,** 820–829 CrossRef Medline
54. Phillips, J. C., Braun, R., Wang, W., Gumbart, J., Tajkhorshid, E., Villa, E., Chipot, C., Skeel, R. D., Kalé, L., and Schulten, K. (2005) Scalable molecular dynamics with NAMD. *J. Comput. Chem.* **26,** 1781–1802 CrossRef Medline

Downloaded from http://www.jbc.org/ by guest on April 10, 2019

ASBMB

55. Brooks, B. R., Brooks C. L., 3rd, Mackerell, A. D., Jr., Nilsson, L., Petrella, R. J., Roux, B., Won, Y., Archontis, G., Bartels, C., Boresch, S., Caflisch, A., Caves, L., Cui, Q., Dinner, A. R., Feig, M., *et al.* (2009) CHARMM: the biomolecular simulation program. *J. Comput. Chem.* **30,** 1545–1614 CrossRef Medline
56. Humphrey, W., Dalke, A., and Schulten, K. (1996) VMD: visual molecular dynamics. *J. Mol. Graph.* **14,** 33–38, 27–28 CrossRef Medline
57. Pettersen, E. F., Goddard, T. D., Huang, C. C., Couch, G. S., Greenblatt, D. M., Meng, E. C., and Ferrin, T. E. (2004) UCSF chimera: a visualization system for exploratory research and analysis. *J. Comput. Chem.* **25,** 1605–1612 CrossRef Medline
58. Jang, H., Muratcioglu, S., Gursoy, A., Keskin, O., and Nussinov, R. (2016) Membrane-associated Ras dimers are isoform-specific: K-Ras dimers differ from H-Ras dimers. *Biochem. J.* **473,** 1719–1732 CrossRef Medline
59. Erdemir, H. H., Li, Z., and Sacks, D. B. (2014) IQGAP1 binds to estrogen receptor-α and modulates its function. *J. Biol. Chem.* **289,** 9100–9112 CrossRef Medline

Downloaded from http://www.jbc.org/ by guest on April 10, 2019

Unraveling the molecular mechanism of interactions of the Rho GTPases Cdc42 and Rac1 with the scaffolding protein IQGAP2

E. Sila Ozdemir, Hyunbum Jang, Attila Gursoy, Ozlem Keskin, Zhigang Li, David B. Sacks and Ruth Nussinov

J. Biol. Chem. 2018, 293:3685-3699.
doi: 10.1074/jbc.RA117.001596 originally published online January 22, 2018

Access the most updated version of this article at doi: 10.1074/jbc.RA117.001596

Alerts:
- When this article is cited
- When a correction for this article is posted

Click here to choose from all of JBC's e-mail alerts

This article cites 59 references, 25 of which can be accessed free at
http://www.jbc.org/content/293/10/3685.full.html#ref-list-1

Downloaded from http://www.jbc.org/ by guest on April 10, 2019